APPLIED CHEMISTRY

# Photocatalytic Degradation of an Odorous Pollutant: 2-Mercaptobenzothiazole in Aqueous Suspension Using $Nd^{3+}-TiO_2$ Catalysts

**F. B. Li,[†,‡] X. Z. Li,[*,†] and K. H. Ng[†]**

*Department of Civil and Structural Engineering, The Hong Kong Polytechnic University, Hong Kong, China, and Guangdong Key Laboratory of Agricultural Environment Pollution Integrated Control, Guangdong Institute of Eco-Environment and Soil Science, Guangzhou, 510650, China*

Photocatalytic degradation of an odorous chemical, 2-mercaptobenzothiazole (MBT), in aqueous suspension was investigated using pure $TiO_2$ and neodymium ion doped $TiO_2$ ($Nd^{3+}-TiO_2$) catalysts. The photocatalytic activity of $Nd^{3+}-TiO_2$ was evaluated in the photocatalytic degradation of MBT in aqueous solution. The experimental results showed that the overall kinetic constant ($k$) of MBT degradation using $Nd^{3+}-TiO_2$ was significantly higher than that using $TiO_2$ and an optimal content of neodymium ion doping was found to be 1.2% (molar ratio). The main intermediates during the MBT degradation were identified by LC/MS−MS, and the final products including sulfate ion, ammonium ion, and nitrate ion were also determined by ion chromatography. Only three main intermediates including benzothiazole, 2-hydroxybenzothiazole, and benzothiazole-2-sulfite were found during the MBT degradation using the $TiO_2$ catalyst, while five main intermediates including benzothiazole, 2-hydroxybenzothiazole, benzothiazole-2-sulfonate, benzothiazole-2-sulfite, and anilinesulfonic acid were found during the MBT degradation using 1.2% $Nd^{3+}-TiO_2$. On the basis of analytical results, a possible pathway of MBT degradation in such a photocatalytic oxidation reaction was proposed and illustrated. It was concluded that the photodegradation of MBT and its intermediates can be enhanced owing to the neodymium ion doping.

## 1. Introduction

2-Mercaptobenzothiazole (MBT) is known as an odorous, toxic, and poorly biodegradable pollutant in our environment. MBT and its derivatives are normally used as biocorrosion inhibitors or antifungal drugs in medical applications, coating agents of metallic surfaces, and also vulcanization accelerators in the rubber industry.[1] In an aquatic environment, MBT has been detected in wastewater effluents from rubber additive manufacturers and tanneries, and often has been found in sewage treatment works and surface water.[2] MBT at a low concentration might inhibit the biodegradation of other organics and the nitrification of wastewater. MBT can be transformed into benzothiazole (BT) in anaerobic media and into 2-hydroxybenzothiazole (OBT) and benzothiazole-2-sulfonate ($BTSO_3$) under aerobic conditions. Consequently, MBT, BT, OBT, and $BTSO_3$ are frequently found in both wastewater and surface water. These semivolatile organic compounds result in some odor problems in wastewater treatment plants.[2,3]

The potential applications of $TiO_2$-based photocatalytic oxidation techniques have attracted much attention because of the complete degradation of toxic and poorly biodegradable organic contaminants into mineral products.[4−6] However, most $TiO_2$ photocatalytic oxidation processes have a limit to their industrialization owing to a low quantum yield (<5%) resulting from fast charge-carrier recombination and low interfacial charge-transfer rates.[4,7] Photocatalytic efficiency of $TiO_2$ catalysts depends strongly upon the relative degree of branching of the reactive electron−hole pairs into interfacial charge-transfer reactions. Therefore, one of the most crucial subjects is to enhance the interfacial charge-transfer reaction. Many research groups have recently improved this technology by doping, implanting, and depositing suitable transitional metal ions,[8,9] noble metals,[10] semiconductor metallic oxides,[11] or nonmetal ions [12,13] into $TiO_2$ structures. Alternatively, $TiO_2$ can also be doped with lanthanide ions/oxides with 4f electron configuration to achieve better photocatalytic reaction performance owing to the enhancement of adsorption behavior. It was reported that lanthanide ions could form complexes with various Lewis bases including acids, amines, aldehydes, alcohols, and thiols in the interaction of the functional groups with their fully empty or partially empty 4f orbitals.[14] Some literature stated that incorporation of lanthanide ions into $TiO_2$ matrix could promote the chemical adsorption of organic substrates onto the photocatalyst surface.[15−17] For example, Xu et al.[18] reported that doping with $La^{3+}$, $Ce^{3+}$, $Er^{3+}$, $Pr^{3+}$, $Gd^{3+}$, $Nd^{3+}$, or $Sm^{3+}$ was beneficial to $NO_2^-$ adsorption. Ranjit and co-workers[14,15] reported the increase of saturated adsorption capacity and adsorption equilibrium constants simultaneously for salicylic acid, *trans*-cinnamic acid, and *p*-chlorophenoxyacetic acid owing to $Eu^{3+}$, $Pr^{3+}$, and $Yb^{3+}$ doping.

In the present study, a series of neodymium ion doped titanium dioxide ($Nd^{3+}-TiO_2$) catalysts were prepared by doping neodymium ion into $TiO_2$ structure with different contents. The photocatalytic activity of the $Nd^{3+}-TiO_2$ catalysts was investigated in the photocatalytic degradation of MBT in

* To whom correspondence should be addressed. Tel.: (852) 2766 6016. Fax: (852) 2334 6389. E-mail: cexzli@polyu.edu.hk.

† The Hong Kong Polytechnic University.

‡ Guangdong Institute of Eco-Environment and Soil Science.

10.1021/ie050139o CCC: $33.50 
Published on Web 12/01/2005

aqueous solution with the purpose of odor control. In the meantime, the main intermediates and products during the photocatalytic degradation of MBT were identified by liquid chromatography/mass spectrometry−mass spectrometry (LC/MS−MS) and ion chromatography (IC) when pure $TiO_2$ and $Nd^{3+}-TiO_2$ catalysts were used.

## 2. Experimental Section

**2.1. Preparation of $Nd^{3+}-TiO_2$ Catalysts.** A series of $Nd^{3+}-TiO_2$ catalysts were prepared by a sol−gel method with the following procedure: 17 mL of tetra-*n*-butyltitanium ($Ti(O-Bu)_4$) was dissolved into 80 mL of absolute ethanol; the $Ti(O-Bu)_4$ solution was added dropwise under vigorous stirring into 100 mL of the mixture solution containing 84 mL of ethanol (95%), 1 mL of 0.1 M $Nd(NO_3)_3$, and 15 mL of acetic acid (99.8%); the resulting transparent colloidal suspension was stirred for 2 h and then aged for 2 days until the formation of gel. The gel was dried at 353 K under vacuum and then ground. The $Nd^{3+}-TiO_2$ powder was then calcined at 773 K for 2 h, and the product $Nd^{3+}-TiO_2$ powder catalyst was eventually obtained in a nominal atomic doping level of 0.2% as 0.2% $Nd^{3+}-TiO_2$. Other $Nd^{3+}-TiO_2$ samples were also prepared according to the above procedure as 0.7% $Nd^{3+}-TiO_2$, 1.2% $Nd^{3+}-TiO_2$, and 2.0% $Nd^{3+}-TiO_2$. All chemicals used in this paper were of analytical grade, and deionized−distilled water was used for solution preparation.

**2.2. Characterization of $Nd^{3+}-TiO_2$ Catalysts.** To determine the crystal phase composition of the prepared $Nd^{3+}-TiO_2$ samples, X-ray diffraction (XRD) measurement was carried out at room temperature using a Rigaku D/MAX-IIIA diffractometer with Cu K$\alpha$ ($\lambda = 0.154\,18$ nm). Accelerating voltage of 30 kV and emission current of 30 mA were applied. The specific surface areas of all samples were measured by the Brunauer−Emmett−Teller (BET) method, in which $N_2$ gas was adsorbed at 77 K using a Carlo Erba sorptometer.

**2.3. Photoreactor System and Experimental Procedures.** A Pyrex cylindrical photoreactor was used in the experiments as shown in the literature,[19] in which an 8-W medium-pressure mercury lamp with an emission peak at 365 nm (The Institute of Electrical Light Source, Beijing) was positioned at the center of the cylindrical vessel and surrounded by a circulating water jacket to control the temperature during reaction. The reaction suspension was prepared by adding 0.25 g of photocatalyst powder into 250 mL of aqueous MBT solution. Prior to photooxidation, the suspension was magnetically stirred in the dark for 30 min to establish adsorption/desorption equilibrium. The aqueous suspension containing MBT and photocatalyst was irradiated under UV illumination with constant aeration. At given time intervals analytical samples were taken from the suspension and immediately centrifuged at 60 rps for 20 min; then they were filtered through a 0.45 $\mu$m Millipore filter to remove the particles. The filtrate was analyzed as required.

**2.4. Analytical Methods.** The MBT concentration in aqueous solution was determined by LC, which consists of a gradient pump (Spectra System P4000), an autosampler (Spectra System Tem AS3000) with a 20 $\mu$L injection loop, a Thermo Ques Hypersil ODS column (C18, 5 $\mu$m, 250 × 4.6 mm i.d.), and a photodiode array UV detector (Spectra System UV6000LP). While a mobile phase (70% methanol and 30% water with 1% acetic acid) was operated at a flow rate of 0.5 mL $min^{-1}$, a maximum absorption wavelength of 323 nm was selected to detect MBT. The intermediates from the MBT photocatalytic degradation were determined by an ion trap mass spectrometer (Finnigan Duo LCQ MS/MS system) with either an electrospray ionization (ESI) probe or an atmospheric pressure chemical ionization (APCI) probe. This mass spectrometer was coupled to the LC. Nitrogen gas was generated by a nitrogen generator (NITROX) and used as both sheath and auxiliary gases. Other optimized instrumental settings included the following: capillary temperature = 433 K, vaporizer temperature = 623 K, discharge current = 10 $\mu$A, discharge voltage = 4.58 kV, and sheath gas flow rate = 60 unit. The LC/MS−MS system was connected to a computer with ICIS software (Xcalibur 1.2) for both instrumental control and data collection. Dissolved organic carbon (DOC) concentration was determined by a TOC analyzer (Shimadzu 5000A) equipped with an ASI-5000 autosampler. The final products of the MBT degradation including sulfate ion ($SO_4^{2-}$), nitrate ion ($NO_3^-$), and ammonium ion ($NH_4^+$) were determined by ion chromatography with a conductivity detector (Shimadzu HIC-6A), in which a Shim-Pack IC-A1 anion column and mobile phase (2.5 mM phthalic acid and 2.4 mM tris(hydroxymethyl)aminomethane) at a flow rate of 1.5 mL $min^{-1}$ were used for determination of $SO_4^{2-}$ and $NO_3^-$, while a Shim-Pack IC-C1 cationic column and mobile phase (5.0 mM nitrate acid) at a flow rate of 1.0 mL $min^{-1}$ were applied for determination of $NH_4^+$.

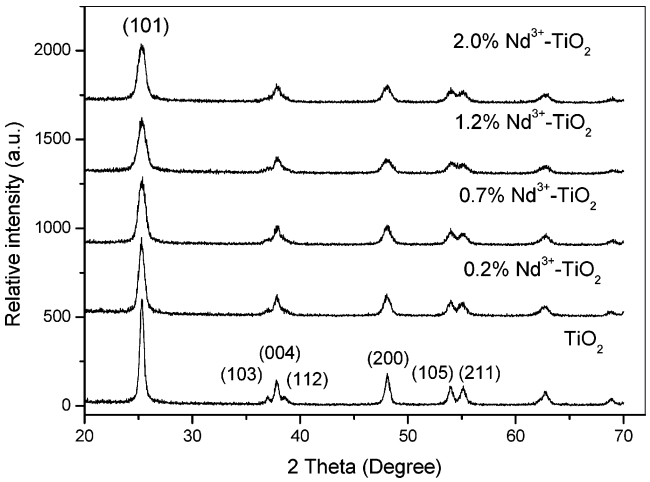


**Figure 1.** XRD photograph of the photocatalysts.

**2.5. Chemicals.** MBT of analytical grade was provided by BDH and used as a model pollutant in the photocatalytic degradation experiments. Other chemicals including benzothiazole (96%), 2-hydroxybenzothiazole (98%), potassium 1,3-benzothiazole (98%), and 2-methylthioaniline (97%) from Aldrich, and aniline-*p*-sulfonic acid (98%) from AJAX Chemicals were used as standards of intermediates in the LC/MS−MS analysis.

## 3. Results and Discussion

**3.1. Crystal Properties and Specific Surface Area.** The prepared $Nd^{3+}-TiO_2$ samples were analyzed by XRD, and the analytical results showed that all samples had a similar pattern of XRD graphs dominated by anatase, as shown in Figure 1. The relative intensity of 101 peaks significantly decreased with the increase of neodymium ion dosage, which indicates that neodymium ion doping may inhibit the phase transformation from amorphous form to anatase in the solid and lead to higher thermal stability. On the basis of XRD data, the crystallite size of the $Nd^{3+}-TiO_2$ samples was calculated using the Scherrer formula. For $TiO_2$, 0.2%, 0.7%, 1.2%, and 2.0% $Nd^{3+}-TiO_2$ catalysts, the crystal size was 32.9, 25.8, 19.2, 19.8, and 17.8 nm, and the specific surface area was 50.2, 67.3, 71.3, 78.5, and 90.8 $m^2\ g^{-1}$, respectively.

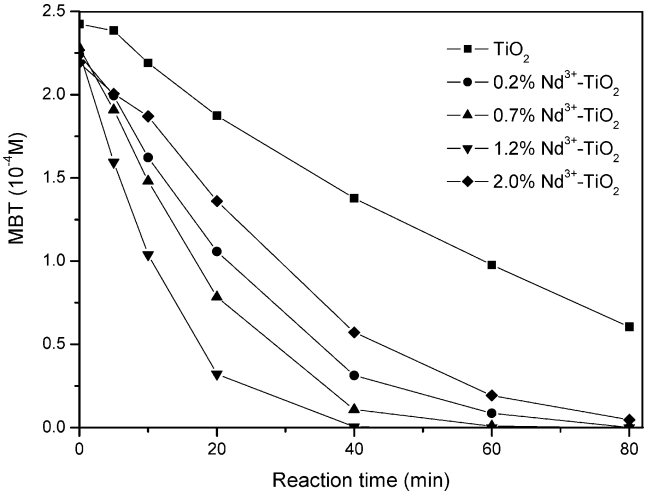


**Figure 2.** MBT photocatalytic degradation with initial concentration of 0.28 mM using different catalysts at pH 6.46.

**Table 1. Overall Kinetic Constants of MBT Degradation with Initial Concentration of 0.28 mM at pH 6.46**

| photocatalysts | $k$ ($min^{-1}$) | correln coeff, $R^2$ |
|---|---|---|
| $TiO_2$ | 0.024 | 0.9985 |
| 0.2% $Nd^{3+}$−$TiO_2$ | 0.0722 | 0.9995 |
| 0.7% $Nd^{3+}$−$TiO_2$ | 0.1106 | 0.9986 |
| 1.2% $Nd^{3+}$−$TiO_2$ | 0.1795 | 0.9956 |
| 2.0% $Nd^{3+}$−$TiO_2$ | 0.061 | 0.9972 |

**3.2. MBT Photocatalytic Degradation.** To evaluate the photocatalytic activity of the $Nd^{3+}$−$TiO_2$ catalysts, a set of tests were carried out to degrade MBT in aqueous suspensions with an initial MBT concentration of 0.28 mM, but using different $Nd^{3+}$−$TiO_2$ catalysts. The experimental results demonstrated that all $Nd^{3+}$−$TiO_2$ catalysts achieved significantly faster MBT degradation than the $TiO_2$ catalyst, as shown in Figure 2. The enhancement of MBT degradation increased initially with the increase of $Nd^{3+}$ content, but decreased as the $Nd^{3+}$ content reached a higher level. The results indicate that 1.2% $Nd^{3+}$−$TiO_2$ catalyst had an optimal $Nd^{3+}$ dosage to achieve the best performance under this experimental condition. The overall kinetic constants, $k$, were calculated, and the results are listed in Table 1. The results show that the 1.2% $Nd^{3+}$−$TiO_2$ catalyst achieved the best performance. To better understand the experimental results, the values of $k$ for 1.2% $Nd^{3+}$−$TiO_2$ and $TiO_2$ are compared. The overall kinetic constant ($k$) of 1.2% $Nd^{3+}$−$TiO_2$ is about 7.5 times of that of $TiO_2$. Our group[17] had reported that the enhancement of MBT photodegradation in $La^{3+}$−$TiO_2$ suspension system resulted from both factors of better adsorption ability and higher photocatalytic activity. In fact, Wang and co-workers[20] had proved the more efficient separation of electron−hole pairs in $Ln^{3+}$−$TiO_2$ particles than in pure $TiO_2$. In the present study, the enhancement of photocatalytic activity of $Nd^{3+}$−$TiO_2$ might be predominantly owing to the higher efficient separation of electron−hole pairs. To a certain degree, the higher content of $Ti^{3+}$ on the $Nd^{3+}$−$TiO_2$ surface compared to that of $TiO_2$ would accelerate the interfacial charge transfer and enhance the photocatalytic activity. However, when the higher dosage of $Nd^{3+}$ leads to an excessive $Ti^{3+}$ content beyond its optimal value, the defect level would become the recombination centers of electron−hole pairs, which result in the decrease of photocatalytic activity.[21]

To investigate the mineralization of MBT, the experiment of MBT degradation with an initial DOC concentration of 20.2 mg $L^{-1}$ was carried out for 80 min. The results of DOC concentration are shown in Figure 3. It was found that the DOC

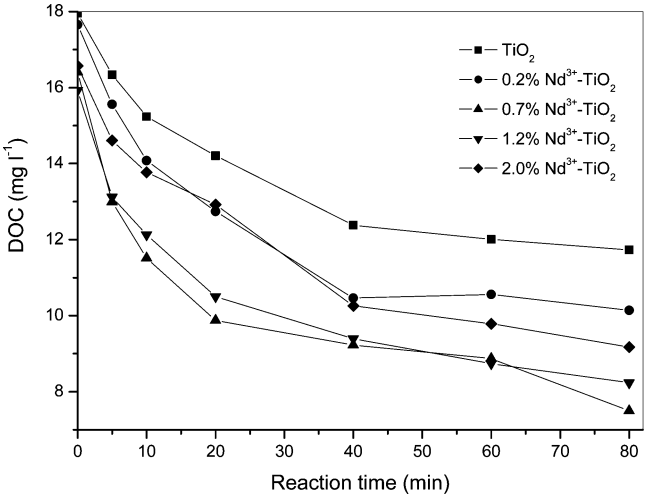


**Figure 3.** DOC removal in MBT photocatalytic degradation using different catalysts under UV irradiation.

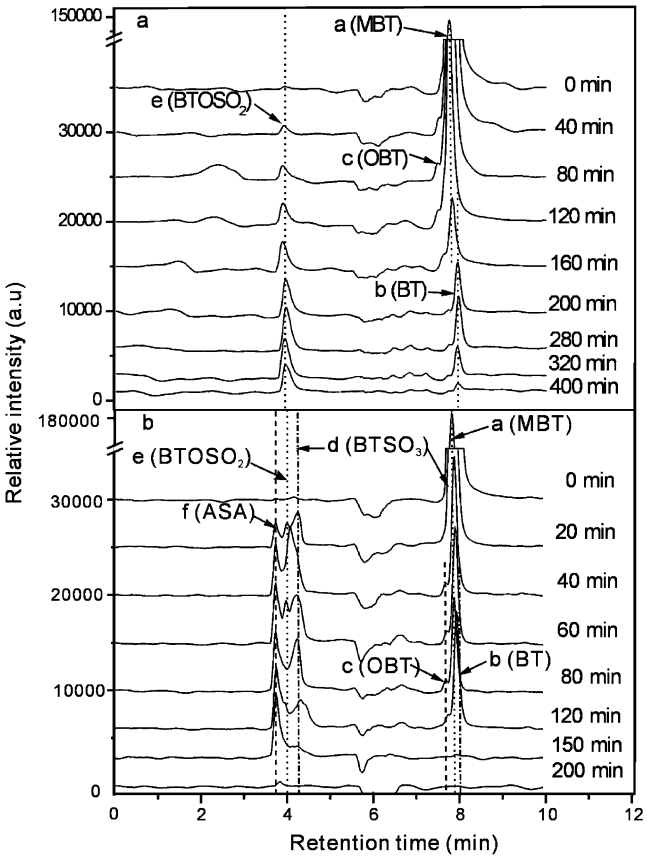


**Figure 4.** Liquid chromatograms of intermediates at different irradiation intervals. LC conditions: mobile phase 70% methanol and 30% water (containing 1% (v/v) acetic acid). Photoreaction conditions: 250 mL of MBT solution with initial concentration of 0.28 mM containing 0.25 g of catalyst under irradiation of a UV lamp (365 nm) and pH 7.15. (a) $TiO_2$; (b) 1.2% $Nd^{3+}$−$TiO_2$.

was removed by 41.9%, 49.8%, 62.8%, 59.2%, and 54.5% for $TiO_2$, 0.2% $Nd^{3+}$−$TiO_2$, 0.7% $Nd^{3+}$−$TiO_2$, 1.2% $Nd^{3+}$−$TiO_2$, and 2.0% $Nd^{3+}$−$TiO_2$, respectively.

**3.3. Intermediates of MBT Degradation.** A number of literature sources reported the determination of intermediates by the LC/MS method.[22−26] In this study, temporal variations of intermediates in the MBT solution during the photoreaction were examined by LC/MS−MS and UV absorption spectrometry. Moreover, some information relevant to MS spectra and

**Table 2. MS−MS Data of the Main Fragments Regarding Peaks a−f in Figure 4**

| peak | retention time (min) | detected ions m/z (% abundance) MS | MS−MS | mol wt | UV peaks (nm) | mol struct | name |
|---|---|---|---|---|---|---|---|
| a | 7.87 | 166 (100) | 166.2 (100), 141 (12), 135 (26), 123 (15), 109 (14.4) | 167.2 | 238, 321 | 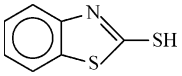 | MBT |
| b | 8.00 | 136.2 (100) | 136.2 (100), 108.2 (61), 92 (25) | 135.2 | 232, 251, 284, 294 | 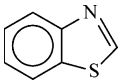 | BT |
| c | 7.80 | 151 (100) | 151.2 (100), 123 (67), 109.3 (11), 96 (58) | 152.2 | 223, 244, 280, 287 | 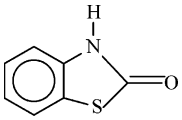 | OBT |
| d | 4.28 | 214 (100) | 214.1 (100), 150.2 (95), 134.2 (35) | 215.1 | 236, 263 | 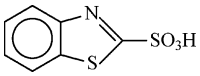 | $BTSO_3$ |
| e | 4.00 | 214 (100) | 214.1 (100), 150.2 (75), 134.2 (30) | 215.1 | 236, 263 | 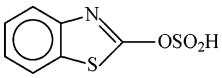 | $BTOSO_2$ |
| f | 3.78 | 174.2 | 174.2 (45), 158.2 (27), 93 (100) | 173.2 | 234, 254 | 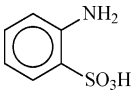 | ASA |

UV−visible absorption spectra was obtained from The National Institute of Standards and Technology (NIST) Library. The samples collected at different reaction times up to 400 min were analyzed by the LC/MS−MS system. The LC of the samples is shown in Figure 4a for $TiO_2$ and in Figure 4b for 1.2% $Nd^{3+}$−$TiO_2$. Other relevant results from the LC/MS−MS analysis are given in Table 2. Obviously, six main peaks at 7.87, 8.00, 7.80, 4.00, 4.28−4.38, and 3.78 min in Figure 4b were identified as "a", "b", "c", "d", "e", and "f", respectively, while only four main peaks at 7.87, 8.00, 7.80, and 3.98 min in Figure 4a were found. In addition, some weak peaks at 4.85, 5.56, and 6.70 min were also found.

On the basis of LC results, it can be seen that when peak a representing MBT decreased against reaction time, other peaks b−f representing five main intermediates increased first and decreased subsequently. To obtain more information about the five intermediates, the UV−visible absorption spectra of peaks b−f for the sample collected at 80 min are expressed in Figure 5. The results illustrate the different patterns of UV absorption spectra and also indicate that there is no significant absorption in the visible region for all the intermediates.

Fiehn et al.[2] reported that the ozonation intermediates of MBT include BT, OBT, and benzothiazole-2-sulfite ($BTOSO_2$). In our investigation, a significant LC peak found at 7.93−8.05 min could be attributable to BT as the first intermediate from the MBT degradation, but the retention time of BT in the LC analysis was very close to that of MBT and the two peaks were not well separated for the samples during 0−40 min reaction. However, the MS−MS analysis showed there was a peak at 8.06 min in ESI SIM MS and APCI MS with a positive ion $m/z = 136.2$, which is very close to the molecular weight of BT (135.2). In addition, the same LC retention time and UV absorption spectra compared to those of BT standard chemical confirmed that BT appeared as the initial intermediate from the MBT degradation and lasted for a long period during the MBT degradation reaction. Peak c occurring at 7.73−7.82 min in LC was attributable to OBT, which was also confirmed by comparing its retention time and UV−visible absorption spectra with the standard OBT chemical. Peak d occurring at 4.17−4.38 min was found to have a negative ion $m/z = 214.1$ corresponding to the peak at 4.40 min in negative ESI MS and the maximum UV absorption peak between 236 and 263 nm. Mohammad et al.[3] reported that $BTSO_3$ was identified as a main intermediate during the MBT photocatalytic degradation with a UV absorption peak at 267 nm. Fiehn et al.[2] reported that the ozonation product of MBT with $m/z = 214$ was $BTOSO_2$, but not $BTSO_3$. In our investigation, the component (peak d) with the UV absorption peak at 263 nm and $m/z = 214.1$ could be either $BTSO_3$ or $BTOSO_2$, since they have the same molecular weight and very similar characteristics in UV−visible absorption spectra, MS, IR spectra, and also NMR spectra. However, it can be found in Figure 5b that a peak occurred at 4.27 min for the sample at the reaction time of 20 min and another peak e occurred at 4.00 min for the sample at the reaction time of 40 min. It has been confirmed that peaks d and e had the same pattern of UV−visible absorption spectra and MS. In addition, the analytical results of the $BTSO_3$ standard showed the LC retention time of 4.28 min and the maximum UV absorption at 263 nm. This information confirmed that peak d occurring at 4.27 min was $BTSO_3$ and peak e occurring at 4.00 min could be $BTOSO_2$.

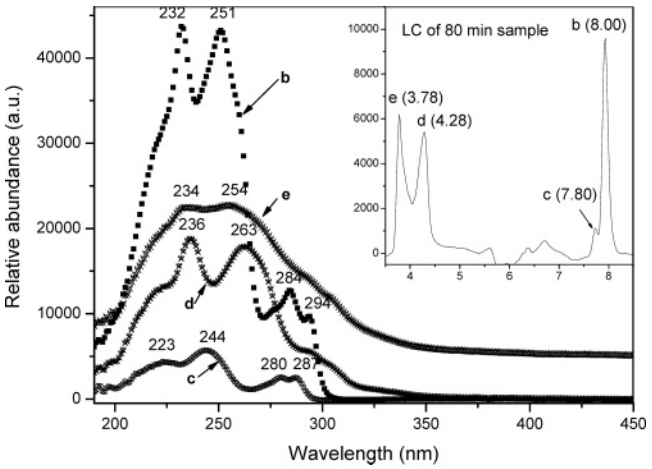


**Figure 5.** UV−visible absorption spectra of intermediates from MBT degradation corresponding to the peaks labeled "a" (7.87 min), "b" (8.00 min), "c" (7.80 min), "d" (4.28 min), and "e" (3.78 min) in the liquid chromatograms of the sample obtained at 80 min as shown in Figure 4a.

Peak f occurring at 3.78 min in Figure 5b seems to be a more polar component than $BTSO_3$, which could be a further product of $BTSO_3$ with a $-SO_3^-$ group. It was found that a significant peak occurring at 3.78 min in the negative ESI full MS had a

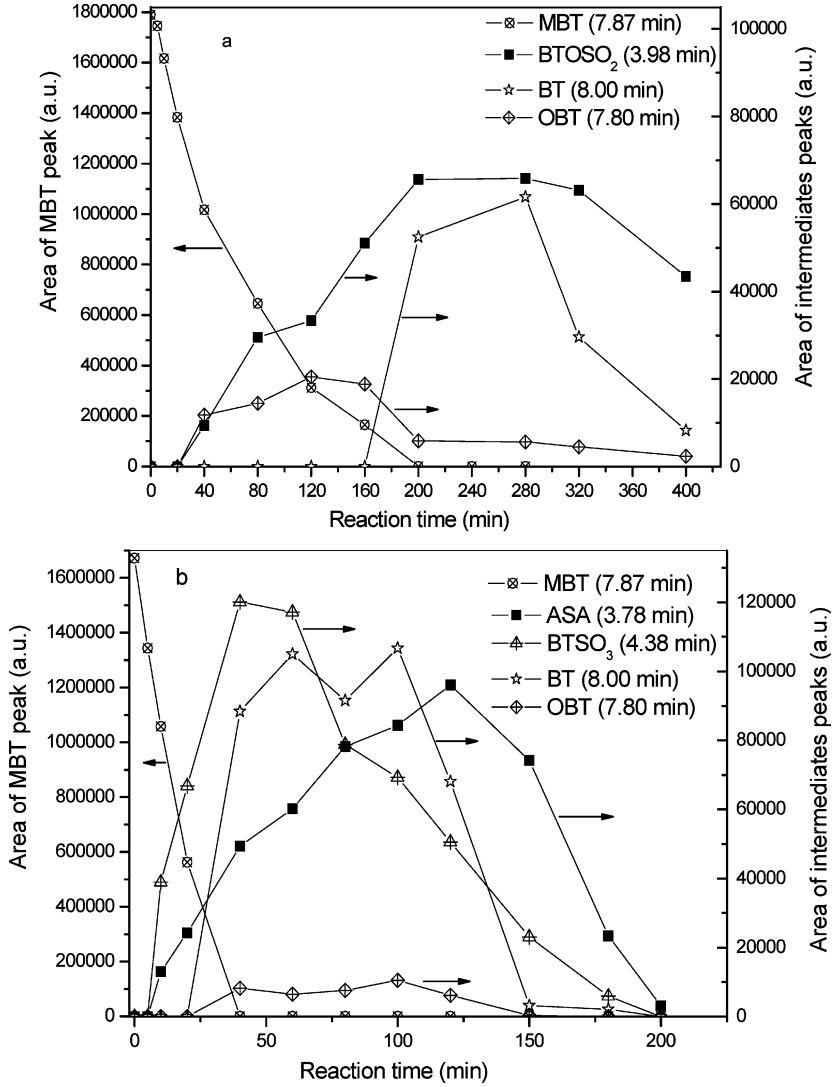


**Figure 6.** Variation of amounts of intermediates during MBT degradation vs reaction time: BT, benzothiazole; OBT, 2(3*H*)-benzothiazolone; $BTSO_3$, benzothiazole-2-sulfonate; $BTOSO_2$, benzothiazole-2-sulfite; and ASA, anilinesulfonic acid. (a) $TiO_2$; (b) 1.2% $Nd^{3+}-TiO_2$.

negative ion $m/z = 172.2$. The MS−MS data of its fragments are listed in Table 2. In addition, the component showed two UV absorption peaks at 234 and 256 nm, respectively. On the basis of above results and the information obtained from the NIST library, it is believed that this component could be anilinesulfonic acid (ASA). Therefore, a standard aniline-*p*-sulfonic acid chemical was used to check the assumption. It showed a retention time of 3.87 min in its LC and one UV absorption peak at 256 nm, which were very close to that of peak f. Once several samples collected at different reaction times were analyzed by LC/MS−MS, it was found that the retention time of peak f shifted from the initial value of 3.78 min to the final value of 3.87 min, when the reaction time lasted up to 200 min. This phenomenon reminded us that the peak f at 3.78 min might be aniline-*o*-sulfonic acid and was further converted to aniline-*p*-sulfonic acid with the retention time of 3.87 min. Additionally, a weak peak at 6.70 min in LC showed two absorption peaks at 235 and 297 nm in its UV absorption spectrum and $m/z = 140.2$ in ESI full MS. It is proposed that this weak peak could be attributed to 2-methylmercaptoaniline (MMA) as another further product of either $BTSO_3$ or $BTOSO_2$.

From the above results, it can be indicated that different intermediates were produced during the MBT degradation when $TiO_2$ or 1.2% $Nd^{3+}-TiO_2$ was used. Only three main intermediates including BT, OBT, and $BTOSO_2$ were identified in the reaction using $TiO_2$, while the five main intermediates (BT, OBT, $BTSO_3$, $BTOSO_2$, and ASA) were identified in the reaction using 1.2% $Nd^{3+}-TiO_2$. Furthermore, variations of their concentrations during the MBT degradation reaction were estimated based on the area of LC; the results are plotted in Figure 6. In Figure 6a, the relative amounts of $BTOSO_2$ and BT increase to their maximum values at 280 min, while that of OBT increases to its maximum value during 120−160 min. In Figure 6b, the results indicate that the relative amounts of BT, OBT, $BTSO_3$, and ASA increase to their maximum values between 40 and 120 min. In the meantime, the LC/MS−MS analysis for the MBT degradation reaction using $Nd^{3+}-TiO_2$ showed a significant difference in terms of intermediates generated during the MBT photoreaction by using $TiO_2$. Moreover, the formation and degradation of intermediates appeared during 40−180 min in the $Nd^{3+}-TiO_2$ suspension while that occurred during 80−400 min in the $TiO_2$ suspension.

**3.4. Products of MBT Degradation.** To evaluate the conversion of organic sulfur and organic nitrogen during the MBT photocatalytic degradation, a set of tests was carried out in the aqueous suspension with the initial concentrations of MBT = 81.6 mg $L^{-1}$, organic sulfur = 31.22 mg $L^{-1}$, and organic nitrogen = 6.83 mg $L^{-1}$ for 240 min, in which seven samples

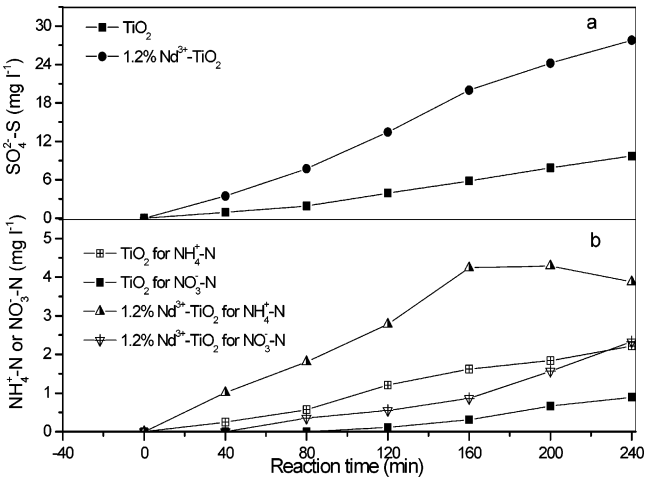


**Figure 7.** Concentration of final products from MBT degradation vs reaction time. (a) $SO_4^{2-}$-S; (b) $NH_4^+$-N and $NO_3^-$-N.

were collected for determination of $SO_4^{2-}$, $NH_4^+$, and $NO_3^-$. The experimental results are shown in Figure 7a for $TiO_2$ and in Figure 7b for 1.2% $Nd^{3+}-TiO_2$.

The experiment demonstrated that the concentration of $SO_4^{2-}$-S during MBT photodegradation reactions using different catalysts ($TiO_2$ and 1.2% $Nd^{3+}-TiO_2$) increased from 0 to 9.69 and 27.8 mg $L^{-1}$, respectively; the concentration of $NH_4^+$-N increased from 0 to 2.22 and 3.88 mg $L^{-1}$, respectively; and the concentration of $NO_3^-$-N increased from 0 to 0.89 and 2.33 mg $L^{-1}$, respectively. The conversion of organic sulfur was achieved by 31% and 89% for $TiO_2$ and 1.2% $Nd^{3+}-TiO_2$, respectively, while the conversion of organic nitrogen was achieved by 45% and 91%, respectively. Although ammonium ion is a product of organic nitrogen in the MBT degradation, it should not be a final product. It is expected that if the experimental time lasted long enough, the ammonium ion would be eventually oxidized to nitrate ion as one of final products.

**3.5. Pathway of MBT Degradation.** On the basis of the above analytical results, a possible pathway of the MBT photocatalytic degradation is proposed and illustrated in Figure 8. The first intermediate, BT, a biodegradable organic, is attacked by hydroxyl radical and then OBT forms. Mercapto group is oxidized and then reacts with OBT before $BTSO_3$ and $BTOSO_2$, major intermediates, form. The S,N-heterocyclic of $BTSO_3$ and $BTOSO_2$ is destroyed and a part of organic sulfur is transformed completely into inorganic sulfur (sulfate) by desulfonation, and MMA forms. This step is very important for the detoxification and deodorization of mercapto compounds and BT derivatives. MMA was oxidized and transformed into ASA including aniline-*o*-sulfonic acid and aniline-*p*-sulfonic acid by demethanation. ASA could be deaminated and organic-N is transformed into inorganic-N ($NH_4^+$ and $NO_3^-$). ASA could also be desulfonated and attacked by hydroxyl radical and then transformed into lower molecular weight organic compounds including organic acids, which are transformed finally into carbon dioxide. More intermediates form and a more complicated pathway is involved in the $Nd^{3+}-TiO_2$ suspension than in $TiO_2$ suspension because of the difference of adsorption sites. The −SH group might only be connected to Ti atom and −Ti−SH complex forms in $TiO_2$ suspension while the −SH group could be connected predominantly to Nd atom and little to Ti atom, and two complexes including −Nd−SH and −Ti−SH formed in $Nd^{3+}-TiO_2$ suspension.

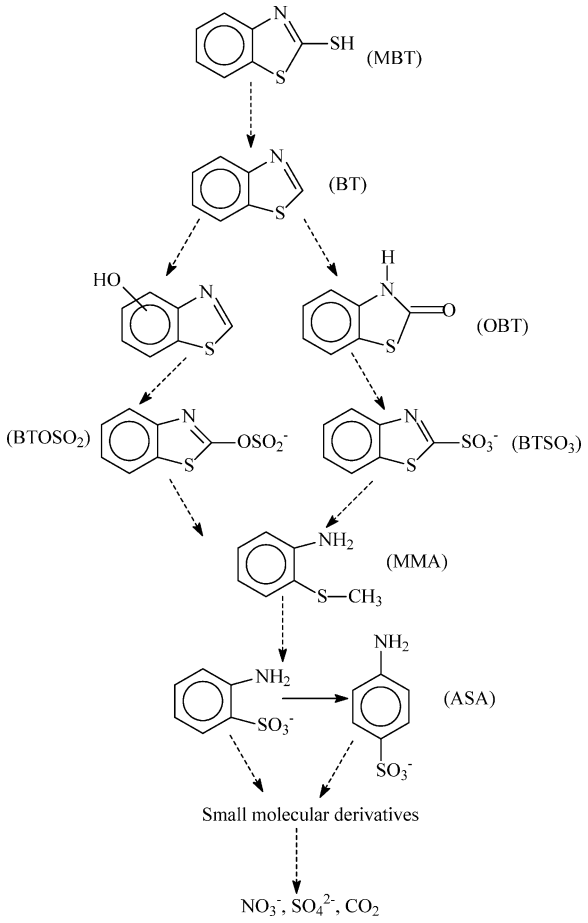


**Figure 8.** A proposed pathway of the MBT photocatalytic degradation.

## 4. Conclusions

The experiments in this study demonstrated that $Nd^{3+}-TiO_2$ catalysts achieved a higher overall kinetic constant for MBT photodegradation than $TiO_2$ catalysts and the optimum dosage of $Nd^{3+}$ was 1.2%. Only three main intermediates of BT, OBT, and $BTOSO_2$ were identified in the reaction using the pure $TiO_2$ catalyst, while five main intermediates of BT, OBT, $BTSO_3$, $BTOSO_2$, and ASA were found in the reaction using 1.2% $Nd^{3+}-TiO_2$ catalyst. It is confirmed that the photocatalytic degradation of MBT and its intermediates were significantly enhanced owing to neodymium ion doping.

## Acknowledgment

The authors are grateful for financial support from The Hong Kong Polytechnic University through a postdoctoral fellowship (Project No. G-YW69/02) and the China National Natural Science Foundation (Project No. 20203007).

## Literature Cited

(1) de Wever H.; de Moor, K.; Verachtert, H. Toxicity of 2-mercaptobenzothiazole towards bacterial growth and respiration. *Appl. Microbiol. Biotechnol.* **1994**, *42*, 631−635.

(2) Fiehn, O.; Wegener, G.; Jochimsen, J.; Jekel, M. Analysis of the ozonation of 2-mercaptobenzothiazole in water and tannery wastewater using sum parameters, liquid- and gas chromatography and capillary electrophoresis. *Water Res.* **1998**, *32*, 1075−1084.

(3) Mohammad, H. H.; Shahram, T.; Bahram, Y. Photocatalytic mineralisation of mercaptans as environmental pollutants in aquatic system using $TiO_2$ suspension. *Appl. Catal., B: Environ.* **2001**, *33*, 57−63.

(4) Fujishima, A.; Rao, N. T.; Tryk, D. A. Titanium dioxide photocatalysis. *J Photochem. Photobiol., C: Photochem. Rev.* **2001**, *1*, 1−21.

(5) Kamat, P. V.; Meisel, D. Nanoscience opportunities in environmental remediation. *C. R. Chim.* **2003**, *6*, 999−1007.

(6) Konstantinou, I. K.; Albanis, T. A. $TiO_2$-assisted photocatalytic degradation of azo dyes in aqueous solution: kinetic and mechanistic investigations: A review. *Appl. Catal., B: Environ.* **2004**, *49*, 1−14.

(7) Linsebiger, A. L.; Lu, G. Q.; Yates, J. T., Jr. Photocatalysis on $TiO_2$ Surfaces: Principles, Mechanisms, and Selected Results. *Chem. Rev.* **1995**, *95*, 735−758.

(8) Choi, W.; Termin, A.; Hoffmann, M. R. The role of metal ion dopants in quantum-sized $TiO_2$: correlation between photoreactivity and charge carrier recombination dynamics. *J. Phys. Chem.* **1994**, *98*, 13669−13679.

(9) Yu, J. G.; Yu, J. C.; Cheng, B.; Hark, S. K.; Iu, K. The effect of $F^-$-doping and temperature on the structural and textural evolution of mesoporous $TiO_2$ powders. *J. Solid State Chem.* **2003**, *174*, 372−380.

(10) Bae, E.; Choi, W. Highly Enhanced Photoreductive Degradation of Perchlorinated Compounds on Dye-Sensitized Metal/$TiO_2$ under Visible Light. *Environ. Sci. Technol.* **2003**, *37*, 147−152.

(11) Li, X. Z.; Li, F. B.; Yang, C. L.; Ge, W. K. Photocatalytic activity of $WO_x$-$TiO_2$ under visible light irradiation. *J. Photochem. Photobiol., A: Chem.* **2001**, *141*, 209−217.

(12) Yu, J. G.; Yu, J. C.; Cheng, B.; Zhao, X. J. Photocatalytic activity and characterization of the sol-gel derived Pb-doped $TiO_2$ thin films. *J. Sol-Gel Sci. Technol.* **2002**, *24*, 39−48.

(13) Zhao, W.; Ma, W.; Chen, C.; Zhao, J.; Shuai, Z. Efficient Degradation of Toxic Organic Pollutants with $Ni_2O_3/TiO_{2-x}B_x$ under Visible Irradiation. *J. Am. Chem. Soc.* **2004**, *126*, 4782−4783.

(14) Ranjit, K. T.; Willner, I.; Bossmann, S. H.; Braun, A. M. Lanthanide Oxide-Doped Titanium Dioxide Photocatalysts: Novel Photocatalysts for the Enhanced Degradation of *p*-Chlorophenoxyacetic Acid. *Environ. Sci. Technol.* **2001**, *35*, 1544−1549.

(15) Ranjit, K. T.; Willner, I.; Bossmann, S. H.; Braun, A. M. Lanthanide Oxide Doped Titanium Dioxide Photocatalysts: Effective Photocatalysts for the Enhanced Degradation of Salicylic Acid and t-Cinnamic Acid. *J. Catal.* **2001**, *204*, 305−311.

(16) Xie, Y. B.; Yuan, C. W. Photocatalysis of neodymium ion modified $TiO_2$ sol under visible light irradiation. *Appl. Surf. Sci.* **2004**, *221*, 17−24.

(17) Li, F. B.; Li, X. Z.; Hou, M. F. Photocatalytic degradation of 2-mercaptobenzothiazole in aqueous $La^{3+}$−$TiO_2$ suspension for odor control. *Appl. Catal., B.: Environ.* **2004**, *48*, 185−194.

(18) Xu, W.; Gao, Y.; Liu, H. Q. The Preparation, Characterization, and their Photocatalytic Activities of Rare-Earth-Doped $TiO_2$ Nanoparticles. *J. Catal.* **2002**, *207*, 151−157.

(19) Li, X. Z.; Liu, H.; Cheng, L. F.; Tong, H. J. Photocatalytic Oxidation Using a New Catalyst-$TiO_2$ Microsphere-for Water and Wastewater Treatment. *Environ. Sci. Technol.* **2003**, *37*, 3989−3994.

(20) Wang, Y. Q.; Cheng, H. M.; Hao, Y. Z.; Ma, J. M.; Li, W. H.; Cai, S. M. Photoelectrochemical properties of metal-ion-doped $TiO_2$ nanocrystalline electrodes. *Thin Solid Films* **1999**, *349*, 120−125.

(21) Hou, M. F.; Li, F. B.; Li, R. F.; Wan H. F.; Zhou, G. Y.; Xie, K. C. Mechanisms of enhancement of photocatalytic properties and activity of $Nd^{3+}$-doped $TiO_2$ for methyl orange degradation. *J. Rare Earths* **2004**, *22*, 542−546.

(22) Liu, G.; Li, X.; Zhao, J.; Hidaka, H.; Serpone, N. Photooxidation Pathway of Sulforhodamine-B. Dependence on the Adsorption Mode on $TiO_2$ Exposed to Visible Light Radiation. *Environ. Sci. Technol.* **2000**, *34*, 3982−3990.

(23) Liu, G.; Wu, T.; Zhao, J.; Hidaka, H.; Serpone, N. Photoassisted degradation of dye pollutants. 8. Irreversible degradation of alizarin red under visible light radiation in air-equilibrated aqueous $TiO_2$ dispersions. *Environ. Sci. Technol.* **1999**, *33*, 2081−2087.

(24) Wu, T.; Lin, T.; Zhao, J.; Hidaka, H.; Serpone, N. $TiO_2$-assisted photodegradation of dyes. 9. Photooxidation of a squarylium cyanine dye in aqueous dispersion under visible light irradiation. *Environ. Sci. Technol.* **1999**, *33*, 1379−1387.

(25) Mónica, A.; Constantine, D. S.; Loreto, L.; Soledad, R.; Dolores, P.-B. $H_2O_2/TiO_2$ photocatalytic oxidation of metol. Identification of intermediates and reaction pathways. *Water Res.* **2002**, *36*, 3582−3592.

(26) Houas, A.; Lachheb, H.; Ksibi, M.; Elaloui, E.; Guillard, C.; Herrmann, J.-M. Photocatalytic degradation pathway of methylene blue in water. *Appl. Catal., B: Environ.* **2001**, *31*, 145−157.

*Received for review* February 4, 2005
*Revised manuscript received* October 23, 2005
*Accepted* November 3, 2005

IE050139O